Inorg. Chem. **2006**, *45*, 7417–7427

Vibrational Spectroscopy and Analysis of Pseudo-tetrahedral Complexes with Metal Imido Bonds

Mark P. Mehn,[†,‡] Steven D. Brown,[†] David M. Jenkins,[†] Jonas C. Peters,*[,†] and Lawrence Que, Jr.*[,‡]

Department of Chemistry and Chemical Engineering, Arnold and Mabel Beckman Laboratories of Chemical Synthesis, California Institute of Technology, Pasadena, California 91125, and Department of Chemistry and Center for Metals in Biocatalysis, 207 Pleasant Street Southeast, University of Minnesota, Minneapolis, Minnesota 55455

Received April 19, 2006

A number of assignments have been previously posited for the metal–nitrogen stretch (ν(M-NR)), the N–R stretch (ν(MN–R)), and possible ligand deformation modes associated with terminally bound imides. Here we examine mononuclear iron(III) and cobalt(III) imido complexes of the monoanionic tridentate ligand [$PhBP_3$] ([$PhBP_3$] = [$PhB(CH_2PPh_2)_3]^-$) to clarify the vibrational features for these trivalent metal imides. We report the structures of [$PhBP_3$]Fe≡N^{t}Bu and [$PhBP_3$]Co≡N^{t}Bu. Pseudo-tetrahedral metal imides of these types exhibit short bond lengths (ca. 1.65 Å) and nearly linear angles about the M–N–C linkages, indicative of multiple bond character. Furthermore, these compounds give rise to intense, low-energy visible absorptions. Both the position and the intensity of the optical bands in the [$PhBP_3$]M≡NR complexes depend on whether the substituent is an alkyl or aryl group. Excitation into the low-energy bands of [$PhBP_3$]Fe≡N^{t}Bu gives rise to two Raman features at 1104 and 1233 cm^{-1}, both of which are sensitive to ^{15}N and ^2H labeling. The isotope labeling suggests the 1104 cm^{-1} mode has the greatest Fe–N stretching character, while the 1233 cm^{-1} mode is affected to a lesser extent by ^{15}N substitution. The spectra of the deuterium-labeled imides further support this assertion. The data demonstrate that the observed peaks are not simple diatomic stretching modes but are extensively coupled to the vibrations of the ancillary organic group. Therefore, describing these complexes as simple diatomic or even triatomic oscillators is an oversimplification. Analogous studies of the corresponding cobalt(III) complex lead to a similar set of isotopically sensitive resonances at 1103 and 1238 cm^{-1}, corroborating the assignments made in the iron imides. Very minimal changes in the vibrational frequencies are observed upon replacement of cobalt(III) for iron(III), suggesting similar force constants for the two compounds. This is consistent with the previously proposed electronic structure model in which the added electron resides in a relatively nonbonding orbital. Replacement of the ^{t}Bu group with a phenyl ring leads to a significantly more complicated resonance Raman spectrum, presumably due to coupling with the vibrations of the phenyl ring. Polarization studies demonstrate that the observed modes have A_1 symmetry. In this case, a clearer resonance enhancement of the signals is observed, supporting a charge transfer designation for the electronic transitions. A series of isotope-labeling experiments has been carried out, and the modes with the greatest metal–nitrogen stretching character have been assigned to peaks at ∼960 and ∼1300 cm^{-1} in both the iron and cobalt [$PhBP_3$]M≡NPh complexes. These results are consistent with a multiple M–N bond for these metal imides.

Introduction

Multiply bonded M═E (or M≡E, where E is C, N, or O) species are key intermediates proposed in a number of group-transfer reactions.[1−13] The diverse reactivity patterns exhibited by these complexes are in part attributed to their

* To whom correspondence should be addressed. E-mail: jpeters@caltech.edu (J.C.P.); que@chem.umn.edu (L.Q.).
† California Institute of Technology.
‡ University of Minnesota.

(1) Doyle, M. P. *Acc. Chem. Res.* **1986**, *19*, 348.
(2) Groves, J. T.; Takahashi, T. *J. Am. Chem. Soc.* **1983**, *105*, 2073.
(3) Nugent, W. A.; Mayer, J. M. *Metal−Ligand Multiple Bonds, The Chemistry of Transition Metal Complexes Containing Oxo, Nitrido, Imido, Alkylidene, or Alkylidyne Ligands*; John Wiley and Sons: New York, 1988.

10.1021/ic060670r CCC: $33.50
Published on Web 08/12/2006

multiple-bond character. Though there are several vibrational studies of d^0-d^2 early transition metal complexes featuring alkylidynes[14−16] and imides,[17−22] systematic vibrational studies using isotope labeling are not as well developed for high d-count complexes featuring metal−nitrogen multiple bonds. There are a few notable instances in which high-valent metal imides have been proposed but were not isolable.[23,24] Recently, a family of high d-count imides of first-row transition metals has been described.[25−33] These imides are rare examples of late metal complexes featuring metal−ligand multiple bond linkages (M=E, M≡E). Prior to their synthesis, late metals featuring such linkages were limited to a few second- and third-row systems.[4,5,19,34−36]

Of the recently prepared first-row imides, those that are pseudo-tetrahedral with approximate 3-fold symmetry can be formally described by a M≡NR bond on the basis of molecular orbital considerations.[26−29,31,37,38] X-ray diffraction studies of these imides reveal short M−N bonds and nearly linear M−N−R angles, consistent with a high metal−nitrogen bond order. With a family of highly colored mononuclear $[PhBP_3]M{\equiv}NR$ (M=Fe, Co; $[PhBP_3]=[PhB(CH_2PPh_2)_3]^-$) complexes available,[26−28,37,38] it is possible to undertake a systematic analysis of the vibrational features of the novel M≡NR fragment in order to clarify assignments made by previous studies.

A number of assignments have been previously posited for the metal−nitrogen stretch ($\nu(M-N\mathrm{R})$), the N−R stretch ($\nu(\mathrm{M}N-R)$), and possible ligand deformation modes associated with terminally bound imides.[16,21,39,40] For example, Dehnicke and co-workers suggested that the $\nu(M-N\mathrm{R})$ stretch (when R is an organic group) should appear between 1200 and 1300 cm^{-1}, whereas $\nu(\mathrm{M}N-R)$ stretches should appear in a range between 850 and 930 cm^{-1}.[39] On the other hand, Osborn and Trogler, upon examination of $Cp^*_2V{=}NPh$, suggested that the $\nu(\mathrm{M}N-R)$ vibrations are between 1200 and 1300 cm^{-1}, whereas the metal−nitrogen stretching modes are between 850 and 1150 cm^{-1}.[40] Alternatively, Hopkins and co-workers pointed out that describing metal−(aryl imido) stretches as symmetric and asymmetric combinations is problematic due to the delocalized nature of the N−C stretch in the parent aniline.[16] In general, vibrational data for metal imides should be interpreted with caution since coupling of the $\nu(M-N\mathrm{R})$ vibration to other modes frequently complicates spectroscopic assignments. Herein, we attempt to clarify the vibrational assignments of the metal imido group, presenting a systematic analysis of the vibrational spectra of a series of trivalent $[PhBP_3]Fe{\equiv}NR$ and $[PhBP_3]Co{\equiv}NR$ complexes aided by isotopic labeling. The collective data presented support a high degree of coupling within the metal(III)−imido linkages and are consistent with multiple bond character as previously ascribed to the metal−imido linkages.[26−29,37]

Experimental Section

General Materials and Procedures. All reagents and solvents were purchased from commercial sources and used as received unless otherwise noted. $Na(^{15}NNN)$, $NH_4(^{15}NO_3)$, aniline-d_7, benzene-d_6, and *tert*-butanol-d_{10} were obtained from Cambridge Isotope Laboratories, Inc. ^{15}N-labeled aniline was obtained from Aldrich. $[PhBP_3]Tl$ was synthesized according to published procedures.[41] The aryl and alkyl azides were prepared according to literature methods.[42−45] $[PhBP_3]FePPh_3$,[27] $[PhBP_3]CoPMe_3$,[26] and $[PhBP_3]CoNCCH_3$[46] were synthesized as previously reported. Unless otherwise noted, solvents were deoxygenated by thoroughly sparging with N_2 gas and then dried by passage through an activated alumina column. Diethyl ether, tetrahydrofuran (THF), petroleum

(4) Glueck, D. S.; Hollander, F. J.; Bergman, R. G. *J. Am. Chem. Soc.* **1989**, *111*, 2719.
(5) Glueck, D. S.; Wu, J.; Hollander, F. J.; Bergman, R. G. *J. Am. Chem. Soc.* **1991**, *113*, 2041.
(6) Woo, L. K. *Chem. Rev.* **1993**, *93*, 1125.
(7) Du Bois, J.; Tomooka, C. S.; Hong, J.; Carreira, E. M. *Acc. Chem. Res.* **1997**, *30*, 364.
(8) Cummins, C. C. *Chem. Commun.* **1998**, *17*, 1777.
(9) Crevier, T. J.; Lovell, S.; Mayer, J. M.; Rheingold, A. L.; Guzei, I. A. *J. Am. Chem. Soc.* **1998**, *120*, 6607.
(10) Mindiola, D. J.; Hillhouse, G. L. *Chem. Commun.* **2002**, 1840.
(11) Lane, B. S.; Burgess, K. *Chem. Rev.* **2003**, *103*, 2457.
(12) Müller, P.; Fruit, C. *Chem. Rev.* **2003**, *103*, 2905.
(13) Waterman, R.; Hillhouse, G. L. *J. Am. Chem. Soc.* **2003**, *125*, 13350.
(14) Foulet-Fonesca, G. P.; Jouan, M.; Dao, N. Q.; Fischer, H.; Schmid, J.; Fischer, E. O. *Spectrochim. Acta* **1990**, *46A*, 339.
(15) Manna, J.; Kuk, R. J.; Dallinger, R. F.; Hopkins, M. D. *J. Am. Chem. Soc.* **1994**, *116*, 9793.
(16) Manna, J.; Dallinger, R. F.; Miskowski, V. M.; Hopkins, M. D. *J. Phys. Chem. B* **2000**, *104*, 10928.
(17) Chambers, O. R.; Harman, M. E.; Rycroft, D. S.; Sharpe, D. W. A.; Winfield, J. M. *J. Chem. Res.* **1977**, *(M)*, 1849.
(18) Nugent, W. A.; Haymore, B. L. *Coord. Chem. Rev.* **1980**, *31*, 123.
(19) Griffith, W. P.; Nielson, A. J.; Taylor, M. J. *J. Chem. Soc., Dalton Trans.* **1988**, 647.
(20) Dehnicke, K.; Strähle, J. *Chem. Rev.* **1993**, *93*, 981.
(21) Korolev, A. V.; Rheingold, A. L.; Williams, D. S. *Inorg. Chem.* **1997**, *36*, 2647.
(22) Heinselman, K. S.; Miskowski, V. M.; Geib, S. J.; Wang, L. C.; Hopkins, M. D. *Inorg. Chem.* **1997**, *36*, 5530.
(23) Jensen, M. P.; Mehn, M. P.; Que, L., Jr. *Angew. Chem., Int. Ed.* **2003**, *42*, 4357.
(24) Lucas, R. L.; Powell, D. R.; Borovik, A. S. *J. Am. Chem. Soc.* **2005**, *127*, 11596.
(25) Mindiola, D. J.; Hillhouse, G. L. *J. Am. Chem. Soc.* **2001**, *123*, 4623.
(26) Jenkins, D. M.; Betley, T. A.; Peters, J. C. *J. Am. Chem. Soc.* **2002**, *124*, 11238.
(27) Brown, S. D.; Betley, T. A.; Peters, J. C. *J. Am. Chem. Soc.* **2003**, *125*, 322.
(28) Betley, T. A.; Peters, J. C. *J. Am. Chem. Soc.* **2003**, *125*, 10782.
(29) Betley, T. A.; Peters, J. C. *J. Am. Chem. Soc.* **2004**, *126*, 6252.
(30) Dai, X.; Kapoor, P.; Warren, T. H. *J. Am. Chem. Soc.* **2004**, *126*, 4798.
(31) Hu, X.; Meyer, K. *J. Am. Chem. Soc.* **2004**, *126*, 16322.
(32) Kogut, E.; Wiencko, H. L.; Zhang, L.; Cordeau, D. E.; Warren, T. H. *J. Am. Chem. Soc.* **2005**, *127*, 11248.
(33) Shay, D. T.; Yap, G. P. A.; Zakharov, L. N.; Rheingold, A. L.; Theopold, K. H. *Angew. Chem., Int. Ed.* **2005**, *44*, 1508.
(34) Hay-Motherwell, R. S.; Wilkinson, G.; Hussain-Bates, B.; Hursthouse, M. B. *J. Chem. Soc., Dalton Trans.* **1992**, 3477.
(35) Hay-Motherwell, R. S.; Wilkinson, G.; Hussain-Bates, B.; Hursthouse, M. B. *Polyhedron* **1993**, *12*, 2009.
(36) Burrell, A. K.; Steedman, A. J. *Organometallics* **1997**, *16*, 1203.
(37) Brown, S. D.; Peters, J. C. *J. Am. Chem. Soc.* **2005**, *127*, 1913.
(38) Thomas, C. M.; Mankad, N.; Peters, J. C. *J. Am Chem. Soc.* **2006**, *128*, 4956.
(39) Dehnicke, K.; Strähle, J. *Angew. Chem., Int. Ed. Engl.* **1981**, *20*, 413.
(40) Osborne, J. H.; Trogler, W. C. *Inorg. Chem.* **1985**, *24*, 3098.
(41) Shapiro, I. R.; Jenkins, D. M.; Thomas, J. C.; Day, M. W.; Peters, J. C. *Chem. Commun.* **2001**, 2152.
(42) Bottaro, J. C.; Penwell, P. E.; Schmitt, R. J. *Synth. Commun.* **1997**, *27*, 1465.
(43) Crivello, J. V. *J. Org. Chem.* **1981**, *46*, 3056.
(44) Hillhouse, G. L.; Bercaw, J. E. *Organometallics* **1982**, *1*, 1025.
(45) Otting, G.; Rumpel, H.; Meschede, L.; Scherer, G.; Limbach, H.-H. *Ber. Bunsen-Ges. Phys. Chem.* **1986**, *90*, 1122.
(46) Jenkins, D. M. Low spin pseudotetrahedral cobalt tris(phosphino)borate complexes. Ph.D. Thesis. California Institute of Technology: Pasadena, CA, 2005; p 230.

ether, benzene, and toluene were typically tested with a standard purple solution of sodium benzophenone ketyl in THF to confirm removal of oxygen and moisture. Dichloromethane was distilled from calcium hydride, and benzene was distilled from sodium/benzophenone prior to use. All metal complex syntheses and manipulations were carried out in a glovebox under a nitrogen atmosphere. All organoimido complexes were stored in the glovebox at −40 °C to slow thermal degradation.

Labeled Compounds. The reagents $N_3C(CD_3)_3$ and 50% α-^{15}N-enriched $N_3{}^t$Bu were prepared according to the method of Bottaro substituting butanol-d_{10} and Na^{15}NNN for the nonisotopically labeled reagents.[42] Due to the nature of this reaction, the resultant azide has a single ^{15}N label either at the α or γ position (in a 1:1 ratio). Generation of the fully ^{15}N-labeled alkyl azide was prohibitively expensive. Diazotization of Ph^{15}NH$_2$ and subsequent reaction with sodium azide yield the desired phenyl azide isotopically ^{15}N-labeled solely at the α-position due to a resonance stabilized cyclic pentazole intermediate.[44,47] The reagent $C_6D_5N_3$ was prepared by diazotization of $C_6D_5ND_2$ followed by an addition of NaN_3.[44,48]

$C_6D_5{}^{15}$NNN. This procedure was based on the method of Crivello.[43] A 50 mL round-bottom flask was charged with benzene-d_6 (6.54 g, 77.7 mmol), $NH_4{}^{15}NO_3$ (0.990 g, 11.1 mmol), and trifluoroacetic anhydride (8.16 g, 38.9 mmol). Chloroform (10 mL) was added, and the reaction was stirred for 2 h. The reaction mixture was combined with 50 mL of water and then extracted with chloroform (3 × 15 mL). The solvent was removed by rotary evaporation, leaving the pure product, $C_6D_5{}^{15}NO_2$ (1.42 g, 99% yield). MS(EI) (*m*/*z*): 129 (M^+). The conversion to the corresponding aniline was based on the method of Limbach.[45] A 300 mL round-bottom flask was charged with $C_6D_5{}^{15}NO_2$ (1.42 g, 11.0 mmol), 10% Pd/C (825 mg), and THF (150 mL). A septa was then attached, and H_2 was allowed to bubble in as the reaction was stirred for 6 h. The THF solution was filtered over a silica plug to remove the Pd/C, and the THF was removed by rotary evaporation. The orange liquid was then put on an alumina column and washed with 200 mL of hexanes to remove a byproduct. The column was then flushed with THF to remove the product. The THF solution was dried with $MgSO_4$ and filtered, and then the THF was removed by rotary evaporation. Trace THF was removed by dissolving the product in hexanes (200 mL) and then removing the solvent through rotary evaporation, leaving the pure product (0.573 g, 52% yield). ^{1}H NMR (C_6D_6, 300 MHz): δ 3.06 (d, $^1J_{H-15N}$ = 70.2 Hz, 2 H). GC/MS (*m*/*z*): 99. $C_6D_5{}^{15}$NNN was prepared via diazotiazation of $C_6D_5{}^{15}NH_2$ as described above.

[PhBP$_3$]Fe≡NR Complexes. [PhBP$_3$]Fe≡N(*p*-tolyl) and [PhBP$_3$]-Fe≡N(1-Ad) were prepared according to the published procedure.[27,37] The other imido complexes (R = ^{t}Bu, Ph) were prepared in a similar fashion through decomposition of the corresponding azide as detailed below.

[PhBP$_3$]Fe≡N^{t}Bu. [PhBP$_3$]FePPh$_3$ (0.200 g, 0.199 mmol) was added to benzene (∼5 mL) with stirring. A benzene solution (1 mL) of *tert*-butylazide (0.0395 g, 0.398 mmol) was added dropwise, during which time the reaction changed color from orange to brown. After 12 h, volatiles were removed under reduced pressure. The resulting crude solids were washed with petroleum ether (3 × 20 mL) and dried under reduced pressure to yield a brown solid (0.113 g, 70%). X-ray-quality crystals were grown via slow evaporation of a benzene solution. ^{1}H NMR (C_6D_6, 300 MHz): δ 19.3 (br, s); 16.5 (br, s); 15.0 (s); 10.6 (t, *J* = 3.0 Hz); 9.61 (t, *J* = 6.8 Hz); 4.92 (d, *J* = 6.6 Hz); 2.39 (t, *J* = 6.6 Hz); −3.67 (br, s). UV−vis (C_6H_6) λ, nm (ϵ, M^{-1} cm^{-1}): 418 (1300); 506 (830). Evans Method (C_6D_6): 1.96 μ_B Anal. Calcd for $C_{49}H_{50}BFeNP_3$: C, 72.43; H, 6.20; N, 1.72. Found: C, 72.26; H, 6.11; N, 1.83.

[PhBP$_3$]Fe≡^{15}N^{t}Bu. [PhBP$_3$]FePPh$_3$ (0.200 g, 0.199 mmol) was added to benzene (∼5 mL) with stirring. A benzene solution (1 mL) of 50% α-^{15}N-enriched *tert*-butylazide (0.0403 g, 0.399 mmol) was added dropwise, during which time the reaction changed color from orange to brown. After 12 h, volatiles were removed under reduced pressure. The resulting crude solids were washed with petroleum ether (3 × 15 mL) and dried under reduced pressure to yield a brown solid (0.070 g, 43%). ^{1}H NMR (C_6D_6, 300 MHz): δ 19.2 (br, s); 16.5 (br, s); 15.0 (s); 10.6 (t, *J* = 6.1 Hz); 9.61 (t, *J* = 6.3 Hz); 4.94 (d, *J* = 7.5 Hz); 2.44 (t, *J* = 6.9 Hz); −3.56 (br, s). This gives a 1:1 mixture of the ^{14}N and ^{15}N imides.

[PhBP$_3$]Fe≡NC(CD$_3$)$_3$. [PhBP$_3$]FePPh$_3$ (0.200 g, 0.199 mmol) was added to benzene (∼5 mL) with stirring. A benzene solution (1 mL) of *tert*-butylazide-d_9 (0.0431 g, 0.399 mmol) was added dropwise, during which time the reaction changed color from orange to brown. After 12 h, volatiles were removed under reduced pressure. The resulting crude solids were washed with petroleum ether (3 × 15 mL) and dried under reduced pressure to yield a brown solid (0.060 g, 37%). ^{1}H NMR (C_6D_6, 300 MHz): δ 19.5 (br, s); 14.9 (s); 10.5 (t); 9.58 (t, *J* = 6.9 Hz); 4.91 (d, *J* = 6.0 Hz); 2.41 (t, *J* = 6.0 Hz); −3.59 (br, s).

[PhBP$_3$]Fe≡NPh. [PhBP$_3$]FePPh$_3$ (0.200 g, 0.199 mmol) was added to benzene (∼5 mL) with stirring. A benzene solution (1 mL) of phenyl azide (0.0475 g, 0.399 mmol) was added dropwise, resulting in a rapid color change from orange to forest green. After 12 h, the reaction was concentrated to a volume of 2 mL under reduced pressure. The addition of petroleum ether (∼18 mL) and stirring for an additional 30 min resulted in the precipitation of green solids, which were isolated on a medium-porosity sintered glass frit. After being washed with additional petroleum ether (3 × 10 mL), the green solids were dried under reduced pressure to yield a pure compound (0.119 g, 72%). Crystals were grown via vapor diffusion of petroleum ether into a benzene solution. ^{1}H NMR (C_6D_6, 300 MHz): δ 14.0 (s); 13.3 (s); 10.1 (br, s); 9.90 (t, *J* = 6.0 Hz); 9.42 (br, s); 9.09 (t, *J* = 7.5 Hz); 5.37 (d, *J* = 7.5 Hz); 3.21 (t, *J* = 6.0 Hz); −0.65 (br, s); −7.19 (s). UV−vis (C_6H_6) λ, nm (ϵ, M^{-1} cm^{-1}): 632 (3000). Evans Method (C_6D_6): 1.87 μ_B Anal. Calcd for $C_{51}H_{46}BFeNP_3$: C, 73.58; H, 5.57; N, 1.68. Found: C, 73.73; H, 5.68; N, 1.76.

[PhBP$_3$]Fe≡^{15}NPh. [PhBP$_3$]FePPh$_3$ (0.300 g, 0.299 mmol) was added to benzene (∼ 5 mL) with stirring. A benzene solution (1 mL) of ^{15}N-phenylazide (0.0712 g, 0.598 mmol) was added dropwise, resulting in a rapid color change from orange to forest green. After 16 h, the reaction was concentrated to a volume of 2 mL under reduced pressure. The addition of petroleum ether (∼18 mL) and stirring for an additional 15 min resulted in the precipitation of green solids, which were isolated on a medium-porosity sintered glass frit. After being washed with additional petroleum ether (3 × 5 mL), the green solids were dried under reduced pressure to yield a pure compound (0.093 g, 37%). ^{1}H NMR (C_6D_6, 300 MHz): δ 14.1 (s); 13.3 (s); 10.0 (br, s); 9.93 (t, *J* = 6.3 Hz); 9.24 (br, s); 9.10 (t, *J* = 7.5 Hz); 5.37 (d, *J* = 6.6 Hz); 3.17 (t, *J* = 6.0 Hz); −0.76 (br, s); −7.54 (s).

[PhBP$_3$]Fe≡NC$_6$D$_5$. [PhBP$_3$]FePPh$_3$ (0.200 g, 0.199 mmol) was added to benzene (∼5 mL) with stirring. A benzene solution (1 mL) of phenylazide-d_5 (0.049 g, 0.399 mmol) was added dropwise, resulting in a rapid color change from orange to forest green. After 16 h, the reaction was concentrated to a volume of 1 mL under reduced pressure. The addition of petroleum ether (∼18 mL) and

(47) Patai, S., Ed. *The Chemistry of the Azido Group*; Interscience Publishers: London, 1971.
(48) Smith, P. A. S.; Brown, B. B. *J. Am. Chem. Soc.* **1951**, *73*, 2438.

stirring for an additional 15 min resulted in the precipitation of green solids, which were isolated on a medium-porosity sintered glass frit. After being washed with additional petroleum ether (3 × 5 mL), the green solids were dried under reduced pressure to yield a pure compound (0.069 g, 41%). ^{1}H NMR (C_6D_6, 300 MHz): δ 13.3 (s); 10.0 (br, s); 9.93 (t, J = 6.9 Hz); 9.10 (t, J = 7.2 Hz); 5.37 (d, J = 6.6 Hz); 3.18 (t, J = 5.4 Hz); −0.72 (br, s).

[PhBP$_3$]Fe≡^{15}NC$_6$D$_5$. [PhBP$_3$]FePPh$_3$ (0.175 g, 0.174 mmol) was added to benzene (∼5 mL) with stirring. A benzene solution (1 mL) of NN^{15}NC$_6$D$_5$ (0.048 g, 0.348 mmol) was added dropwise, resulting in a rapid color change from orange to forest green. After 5 h, the reaction was concentrated to a volume of 2 mL under reduced pressure. The addition of petroleum ether (∼18 mL) and stirring for an additional 30 min resulted in the precipitation of green solids, which were isolated on a medium-porosity sintered glass frit. After being washed with additional petroleum ether (3 × 5 mL), the green solids were dried under reduced pressure. Vapor diffusion of petroleum ether into a concentrated benzene solution of the product yields a pure compound (0.010 g, 7%).^{1}H NMR (C_6D_6, 300 MHz): δ 13.3 (s); 10.0 (br, s); 9.92 (t, J = 6.9 Hz); 9.10 (t, J = 7.2 Hz); 5.37 (d, J = 6.6 Hz); 3.17 (t, $J \approx$ 5 Hz); −0.74 (br, s).

[PhBP$_3$]Co≡NR Complexes. [PhBP$_3$]Co≡NPh, [PhBP$_3$]Co≡^{15}NPh, and [PhBP$_3$]Co≡N(*p*-tolyl) were prepared according to the published procedures.[26] The other imido complex (R = ^{t}Bu) was prepared in a similar fashion through decomposition of the corresponding azide. The syntheses of the isotopically labeled complexes are detailed below.

[PhBP$_3$]Co≡N^{t}Bu. A benzene (2 mL) solution of N$_3$^{t}Bu (114 mg, 1.16 mmol) was added to a stirring benzene (8 mL) solution of [PhBP$_3$]CoPMe$_3$ (159 mg, 0.194 mmol). The reaction mixture was stirred and heated to 55 °C for 6 h. After cooling to room temperature, the reaction mixture was frozen and dried to a brown powder by lyophilization. This powder was then washed with petroleum ether (2 × 10 mL) and dried to afford the product (41 mg, 26% yield). The product can be crystallized by vapor diffusion of petroleum ether into benzene. ^{1}H NMR (C_6D_6, 300 MHz): δ 8.12 (*d*, J = 6.9 Hz, 2 H), 7.70 (*t*, J = 7.8 Hz, 2 H), 7.66 (*m*, 12 H), 7.46 (*t*, J = 7.2 Hz, 1 H), 6.78 (*m*, 18 H), 1.58 (*s*, 9 H), 1.49 (*s* br, 6 H). ^{31}P{1H} NMR (C_6D_6, 121.4 MHz): δ 70 (br). UV−vis (C_6H_6) λ_{max}, nm: 480 (1500).

[PhBP$_3$]Co≡NC(CD$_3$)$_3$. A benzene (2 mL) solution of N$_3$C(CD$_3$)$_3$ (28.2 mg, 0.260 mmol) was added to stirring benzene (8 mL) solution of [PhBP$_3$]CoPMe$_3$ (107 mg, 0.130 mmol), and the solution was heated to 50 °C for 20 h. The brown solution was then frozen and lyophilized, and the brown powder was washed with petroleum ether (10 mL). The petroleum ether solution was dried in vacuo and then crystallized by mixing benzene and petroleum ether and standing at −35 °C, yielding pure brown crystals (69.2 mg, 64% yield). ^{1}H NMR (C_6D_6, 300 MHz): δ 8.12 (d, J = 6.9 Hz, 2 H), 7.71 (t, J = 7.5 Hz, 2 H), 7.66 (m, 12 H), 7.47 (t, J = 6.9 Hz, 1 H), 6.78 (m, 18 H), 1.51 (br s, 6 H). ^{31}P{^{1}H} NMR (C_6D_6, 121.4 MHz): δ 69 (br s).

[PhBP$_3$]Co≡^{15}N^{t}Bu. The protocol for [PhBP$_3$]CoNC(CD$_3$)$_3$ was followed using 50% α-^{15}N-enriched N$_3$^{t}Bu (27.4 mg, 0.275 mmol) and [PhBP$_3$]CoPMe$_3$ (113 mg, 0.138 mmol). Brown crystals were isolated in 74% yield. ^{1}H NMR (C_6D_6, 300 MHz): δ 8.10 (d, J = 6.9 Hz, 2 H), 7.65 (m, 14 H), 7.46 (t, J = 6.9 Hz, 1 H), 6.78 (m, 18 H), 1.58 (br s, 6 H). ^{31}P{^{1}H} NMR (C_6D_6, 121.4 MHz): δ 70 (br s). This gives a 1:1 mixture of the ^{14}N and ^{15}N imides.

[PhBP$_3$]Co≡NC$_6$D$_5$. A benzene (4 mL) solution of N$_3$(C_6D_5) (37.0 mg, 0.297 mmol) was added to a stirring benzene (8 mL) solution of [PhBP$_3$]CoNCCH$_3$ (212 mg, 0.270 mmol). Vigorous bubbling occurred immediately after the addition of the azide solution, and the reaction mixture turned red. The solution was stirred for 1 h and then frozen and lyophilized. The red powder was then washed with petroleum ether (3 × 10 mL), dissolved in benzene, and crystallized by vapor diffusion of petroleum ether giving red crystals (150 mg, 64% yield). ^{1}H NMR (C_6D_6, 300 MHz): δ 8.13 (d, J = 6.9 Hz, 2 H), 7.74 (m, 14 H), 7.49 (t, J = 6.9 Hz, 1 H), 6.74 (m, 18 H), 1.48 (br s, 6 H). ^{31}P{^{1}H} NMR (C_6D_6, 121.4 MHz): δ 63 (br). ESI/MS (*m*/*z*): 841 (M + H$^+$) UV−vis (C_6H_6) λ_{max}, nm (ϵ): 412, 533.

[PhBP$_3$]Co≡^{15}NC$_6$D$_5$. A benzene (2 mL) solution of NN^{15}N(C_6D_5) (36.6 mg, 0.292 mmol) was added to a stirring benzene (10 mL) solution of [PhBP$_3$]CoPMe$_3$ (120 mg, 0.146 mmol). Vigorous bubbling occurred immediately after the addition of the azide solution, and the reaction mixture turned red. The solution was stirred for 2 h and then frozen and lyophilized. The red powder was then washed with petroleum ether (3 × 15 mL), dissolved in benzene, and crystallized by vapor diffusion of petroleum ether giving red crystals (43 mg, 35% yield). ^{1}H NMR (C_6D_6, 300 MHz): δ 8.13 (d, J = 6.9 Hz, 2 H), 7.74 (m, 14 H), 7.49 (t, J = 6.9 Hz, 1 H), 6.74 (m, 18 H), 1.48 (br s, 6 H). ^{31}P{^{1}H} NMR (C_6D_6, 121.4 MHz): δ 66 (br). UV−vis (C_6H_6) λ_{max}, nm (ϵ): 416, 537.

Physical Methods. UV−vis spectra were recorded on a HP 8453A diode-array spectrometer at room temperature. The Raman samples were prepared, loaded onto the sample holder, and frozen on the coldfinger in the glovebox. Resonance Raman spectra were collected on an Acton AM-506 spectrometer (1200 groove grating) using a Kaiser Optical holographic super-notch filter with a Princeton Instruments liquid-N_2-cooled (LN-1100PB) CCD detector with a 4 cm^{-1} spectral resolution. The laser excitation lines were obtained with a Spectra Physics 2030-15 argon ion laser and a 375B CW dye (Rhodamine 6G), or a Spectra Physics BeamLok 2060-KR-V krypton ion laser. The Raman frequencies were referenced to indene, and the entire spectral range was obtained by collecting spectra at several different frequency windows and splicing the spectra together. The spectra were obtained at 77 K using a backscattering geometry on samples frozen on a gold-plated copper coldfinger in thermal contact with a Dewar containing liquid N_2. The power recorded at the laser for each sample was 100 mW. After the beam was passed through a pre-monochromator to eliminate plasma lines and was focused onto the sample, the incident power was much lower (usually near 20 mW). No photobleaching was observed upon repeated scans. Furthermore, the excitation profiles showed no evidence of bleaching upon returning to the original excitation wavelength. Typical accumulation times were 16−32 min per frequency window. Curve fits (Gaussian functions) and baseline corrections (polynomial fits) were carried out using Grams/32 Spectral Notebase Version 4.04 (Galactic). Efforts were made to retain the width and position of the natural-abundance samples, especially in the samples of the ^{15}N alkyl imides. For example, the same peak width was used for the ^{15}N peaks and the position was optimized. Excitation profiles were constructed by comparing peak area to the nonresonance enhanced vibration of dichloromethane at 1410 cm^{-1}. X-ray diffraction studies were carried out in the Beckman Institute Crystallographic Facility on a Bruker Smart 1000 CCD diffractometer. Further details regarding X-ray diffraction data collection and solution of the diffraction patterns are available in the Supporting Information.

Results

The structures of several mononuclear trivalent low-spin iron and cobalt imides were reported previously (e.g., [PhBP$_3$]-

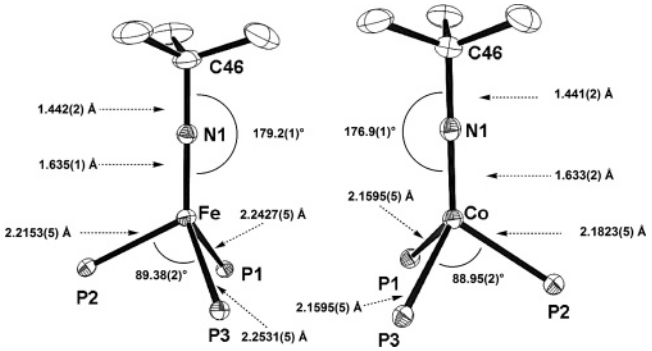

Figure 1. Solid-state molecular structures of $[PhBP_3]Fe{\equiv}N^tBu$ (left) and $[PhBP_3]Co{\equiv}N^tBu$ (right). Only the phosphorus atoms of the $[PhBP_3]$ ligand are included in this figure for clarity. In the case of the cobalt imide, the 1.5 co-crystallized benzene molecules have also been omitted for clarity.

$Fe^{III}{\equiv}N(p\text{-tolyl})$, $[PhBP_3]Fe^{III}{\equiv}N(1\text{-Ad})$, and $[PhBP_3]Co^{III}{\equiv}N(p\text{-tolyl})$.[26−28,37,46] These complexes exhibit short metal−nitrogen bond lengths (Fe−N(*p*-tolyl) = 1.6578(2) Å, Fe−N(1-Ad) = 1.641(2) Å, Co−N(*p*-tolyl) = 1.658(2) Å, and Co−N^{t}Bu = 1.633(2) Å) with nearly linear M−N−C angles (169.96(2)°, 176.33(1)°, 169.51(2)°, and 176.68(13)°, respectively). The alkyl-substituted imido complexes appear to show less of a deviation from linearity. Here we report the structures of $[PhBP_3]Fe{\equiv}N^tBu$ and $[PhBP_3]Co{\equiv}N^tBu$ (Figure 1). The structures of these alkyl imides are consistent with those previously reported.[26−28,37,46] In both the iron and cobalt imides, the metal center exhibits a pseudo-tetrahedral geometry (P_xMP_y angles near 90°), the metal−nitrogen bond distances are short (1.63−1.64 Å), and the MNC bond angles are nearly linear. A similar geometry is observed when the more electron-releasing isopropyl-substituted ligand $[PhBP^{iPr}_3]$ is used to support a metal imide. For example, the structure of $[PhBP^{iPr}_3]Fe^{III}{\equiv}N(1\text{-Ad})$ exhibits an Fe−N distance of 1.638(2) Å and an Fe−N−C angle of 176.0(2)°.[28] This is also similar to the distances and angles observed for the terminal imide in the mixed-valent cluster $[Fe_4(\mu_3\text{-}N^tBu)_4(N^tBu)Cl_3]$ reported by Lee and co-workers (Fe−N = 1.635(4) Å, Fe−N−C = 178.6(3)°).[49]

Optical Properties. Rigorous fitting and interpretation of the optical spectra of these d^6 and d^5 imides will be the subject of a separate study. It is nonetheless useful to provide a qualitative description of their respective optical spectra here. We have therefore acquired the optical spectra of these trivalent cobalt and iron imides. $[PhBP_3]Fe{\equiv}NPh$ is forest green in color. This d^5 iron imide exhibits a broad absorption band near 630 nm (ϵ = 3300 M^{-1} cm^{-1}) and a shoulder at higher energy near 400 nm (ϵ = 7000 M^{-1} cm^{-1}) (Figure 2A, Table 1). Replacement of the aryl substituent with an alkyl group results in lower extinction coefficients and significantly blue-shifted absorption maxima (Figure 2C). These intensely colored complexes exhibit rich electronic spectra with multiple high-intensity bands.

The analogous low-spin d^6 cobalt complex $[PhBP_3]Co{\equiv}NPh$ is red-brown in color and exhibits multiple intense bands (Figure 2B, λ_{max} = 534, 406 nm). A broad feature can also be observed (which terminates at ∼750 nm). The introduction of ring substituents does not affect the wavelengths of the observed transitions in a systematic fashion; both electron-releasing (−CH_3, −NMe_2) and electron-withdrawing substituents (−CF_3) result in red-shifts, and the shifts are relatively small (Table 1). The spectrum of the cobalt alkyl imide also exhibits a lower extinction coefficient (Figure 2D).

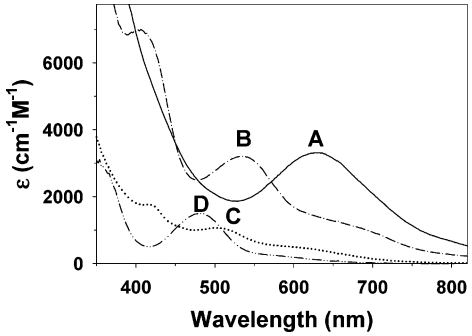

Figure 2. Electronic spectra of $[PhBP_3]M{\equiv}NR$ complexes. All spectra were recorded at room temperature in CH_2Cl_2. (A) $[PhBP_3]Fe{\equiv}NPh$ (−); (B) $[PhBP_3]Co{\equiv}NPh$ (− · −). (C) $[PhBP_3]Fe{\equiv}N^tBu$ (···); and(D) $[PhBP_3]$-$Co{\equiv}N^tBu$ (−··−).

Table 1. Summary of $[PhBP_3]M{\equiv}NR$ Properties and Comparisons

compound	color	λ_{max}, nm (ϵ, cm^{-1} M^{-1})	ref
	Aryls		
$Cp^*_2V{\equiv}NPh$	dark green	−	40
$[PhBP_3]Fe{\equiv}N(p\text{-tolyl})$	forest green	400 (sh, 7000), 640 (3300)	27
$[PhBP_3]Fe{\equiv}NPh$	forest green	400 (sh, 7000), 630 (3300)	
$[PhBP_3]Co{\equiv}NC_6H_4NMe_2$	dark red	454 (10500), 543 (9900)	
$[PhBP_3]Co{\equiv}N(p\text{-tolyl})$	dark red	420 (7000), 538 (3500)	26
$[PhBP_3]Co{\equiv}NPh$	dark red	406 (7000), 534 (3210)	26
$[PhBP_3]Co{\equiv}NC_6H_4{-}CF_3$	dark red	422 (6800), 549 (4500)	
	Alkyls		
$[Fe_4(\mu_3\text{-}N^tBu)_4(N^tBu)Cl_3]$	black	−	49
$[PhBP_3]Fe{\equiv}N^tBu$	brown	418 (1300), 506 (830)	
$[PhBP_3]Fe{\equiv}N(1\text{-Ad})$	brown	422 (1600), 510 (1050)	37
$[PhBP_3]Co{\equiv}N^tBu$	red-brown	480 (1500)	46
$\{[PhBP_3]Fe{\equiv}N(1\text{-Ad})\}^-$	brown	510 (2110), 600 (815)	37

Metal−Imido Vibrational Features. Excitation of $[PhBP_3]Fe{\equiv}N^tBu$ with 406.7 nm light affords a rich Raman spectrum (Figure 3A, Table 2). The Raman spectrum shows bands at 519, 577, 998, 1028, 1103, and 1233 cm^{-1}. On the basis of the isotope-labeling experiments described below, three features at 519, 1104, and 1233 cm^{-1} can be attributed to the $Fe^{III}{\equiv}N^tBu$ fragment, though there is not a substantial resonance enhancement of the 519 cm^{-1} band (Figure 4). The spectra of the isotopically labeled compounds show some variation in the band areas from the natural-abundance samples. This is not uncommon because the composition of the normal mode changes upon isotopic substitution. The peak widths of the natural abundance sample spectra were kept constant when fitting the ^{15}N spectra. The 519 cm^{-1} feature is insensitive to ^{15}N substitution but displays a 6 cm^{-1} downshift upon deuteration of the *tert*-butyl group; this vibration must involve deformation of the ^{t}Bu group. As discussed in the Experimental Section, the maximum incorporation of ^{15}N label is 50%, and analysis of a 1:1 mixture of labeled and unlabeled complex shows that both bands at 1104 and 1233 cm^{-1} are sensitive to ^{15}N substitution (downshifting by 20 and 5 cm^{-1}, respectively, Figure 3B).

(49) Verma, A. K.; Nazif, T. N.; Achim, C.; Lee, S. C. *J. Am Chem. Soc.* **2000**, *122*, 11013.

Table 2. Metal−Imido Vibrational Data (in CH_2Cl_2 unless Noted Otherwise)

compound	observed vibrational frequencies (cm^{-1})													ref
Iron N-Alkyls														
$[PhBP_3]Fe{\equiv}N^tBu$	519				1104		1233							
$[PhBP_3]Fe{\equiv}^{15}N^tBu$	520				1084		1228							
$[PhBP_3]Fe{\equiv}N^tBu\text{-}d_9$	513				1096		1219							
$[PhBP_3]Fe{\equiv}N(1\text{-Ad})$					1097		1225							
$[Fe_4(\mu_3\text{-}N^tBu)_4(N^tBu)Cl_3]^a$			955	1021/1068	1111	1167	1214	1262	1361	1384	1461			49
Cobalt N-Alkyls														
$[PhBP_3]Co{\equiv}N^tBu$	521	577			1103		1238							
$[PhBP_3]Co{\equiv}^{15}N^tBu$	521	578			1084									
$[PhBP_3]Co{\equiv}N^tBu\text{-}d_9$	529	549			1100		1226							
Early Metal N-Alkyls														
$Ta(N^tBu)Cl_3(dme)$							1275					1586		21
Iron N−Aryls														
$[PhBP_3]Fe{\equiv}NPh$		547	672		958	995	1163	1292	1309	1339		1466	1573	
$[PhBP_3]Fe{\equiv}^{15}NPh$		538	670		946	993	1163	1277	1294	1339		1465	1572	
$[PhBP_3]Fe{\equiv}NPh\text{-}d_5$		532	661	856 936	962			1249	1272		1362	1368	1536	
$[PhBP_3]Fe{\equiv}^{15}NPh\text{-}d_5$		524	649	855 932	959			1236	1247		1357	1361	1536	
$[PhBP_3]Fe{\equiv}N(p\text{-tolyl})$		547	658		962	1007	1167	1281	1305			1482	1589	
Cobalt N-Aryls														
$[PhBP_3]Co{\equiv}NPh$		545			956	995	1163	1307	1332			1464	1571	
$[PhBP_3]Co{\equiv}NPh^b$									1340					26
$[PhBP_3]Co{\equiv}^{15}NPh$		540			944	992	1163	1295	1313			1465	1572	
$[PhBP_3]Co{\equiv}NPh\text{-}d_5$		490		856	934	959		1252	1264			1368	1531/1535	
$[PhBP_3]Co{\equiv}^{15}NPh\text{-}d_5$		489		856	934	956		1235/1242	1257			1361	1531/1536	
$[PhBP_3]Co{\equiv}N(p\text{-tolyl})$		546			959	1006	1168	1317				1476	1589	
Early Metal N-Aryls														
$Cp^*_2V{\equiv}NPh^b$					934			1330						40
$Cp^*_2V{\equiv}^{15}NPh^b$					923			1307						40
$Cp^*_2V{\equiv}N(C_6F_5)^b$					968			1303						40
$Cp^*_2V{\equiv}N(2,6\text{-}Me_2C_6H_3)^b$					940			1293						40
$Cp^*_2V{\equiv}N(2\text{-biphenyl})^b$					937			1303						40
$[\{W(NPh)Cl_4\}_2]$		540	683	844	995	998	1173	1270	1349			1479	1583	19
$[\{W(^{15}NPh)Cl_4\}_2]$		540	678	844	983	995	1172	1270	1332			1477	1581	19
$[Ta(NPh)(Cl)_3(dme)]$		558	608	858	958	998	1177	1259	1301	1357		1433	1586	22
$Ta(NPh)Cl_3$			710		993		1076	1211				1475	1645	21
$[Nb(NPh)(Cl)_3(dme)]$		557	610	858	953	993	1178	1260	1291	1334		1427	1585	22

[a] IR data taken KBr, new assignments. [b] IR data taken in Nujol.

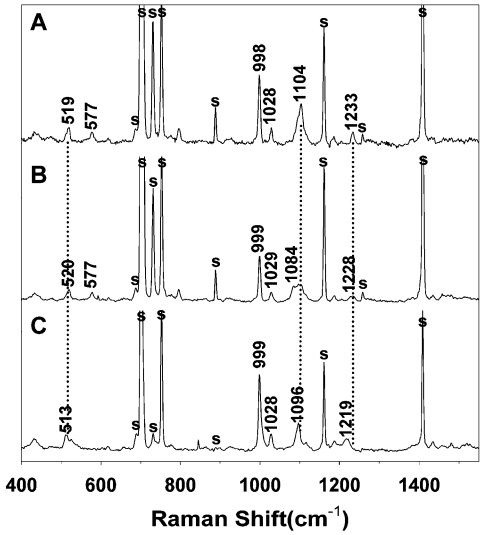

Figure 3. Raman spectra of (A) $[PhBP_3]Fe{\equiv}N^tBu$, (B) 1:1 $[PhBP_3]Fe{\equiv}^{15}N^tBu$: $[PhBP_3]Fe{\equiv}^{14}N^tBu$, and (C) $[PhBP_3]Fe{\equiv}N^tBu\text{-}d_9$ in CH_2Cl_2. All spectra were obtained at 77 K using a backscattering geometry (406.7 nm excitation). Peaks due to solvent are marked with an 's'.

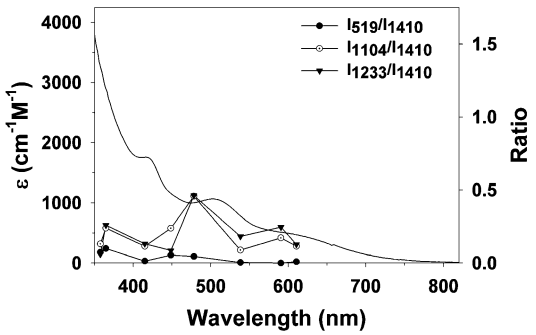

Figure 4. Electronic spectrum of $[PhBP_3]Fe{\equiv}N^tBu$ in CH_2Cl_2 recorded at room temperature, and resonance Raman excitation profiles for the bands assigned to the compound.

Since a simple iron−nitrogen harmonic oscillator at 1104 cm^{-1} would downshift by 30 cm^{-1}, the 1104 cm^{-1} mode must possess significant Fe−N character. The fact that deuteration of the ^{t}Bu group results in an 8 cm^{-1} downshift of this mode suggests some admixture with *tert*-butyl deformation mode(s) (Figure 3C). Deuteration affects the 1233 cm^{-1} feature to a greater extent (14 cm^{-1} downshift) than the 1104 cm^{-1} band, while ^{15}N labeling engenders only a 5 cm^{-1} downshift. The excitation profile of $[PhBP_3]Fe{\equiv}N^tBu$ shows that the vibrations at 1104 and 1233 cm^{-1} are weakly enhanced (Figure 4). Analogous modes appear at 1097 and 1225 cm^{-1} in the adamantyl-substituted complex $[PhBP_3]Fe{\equiv}N(1\text{-Ad})$ (Table 2).

Excitation of the corresponding cobalt complexes with 457.9 nm light affords similar vibrational features (Figure

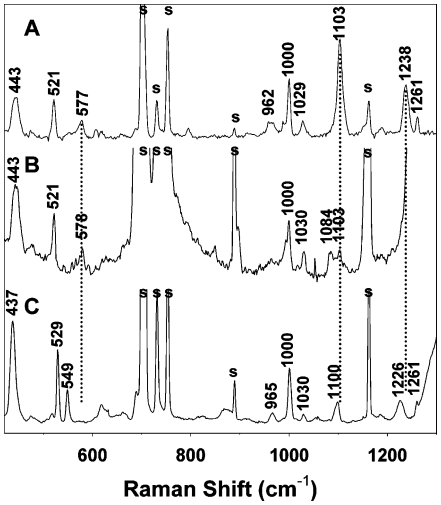

Figure 5. Raman spectra of (A) $[PhBP_3]Co{\equiv}N^tBu$, (B) 1:1 $[PhBP_3]Co{\equiv}{}^{15}N^tBu$: $[PhBP_3]Co{\equiv}N^tBu$, and (C) $[PhBP_3]Co{\equiv}N^tBu$-d_9 in CH_2Cl_2. All spectra were obtained at 77 K using a backscattering geometry (457.9 nm excitation). Peaks due to solvent are marked with an 's'.

5, Table 2). The cobalt complexes are relatively insensitive to excitation wavelength and show very minimal resonance enhancement. The Raman spectrum of $[PhBP_3]Co{\equiv}N^tBu$ displays a number of bands that are sensitive to isotopic substitution, namely the features at 443, 521, 577, 1103, and 1238 cm^{-1}. The features at 443, 521, and 577 cm^{-1} show no sensitivity to ^{15}N labeling; however, they are affected by deuteration exhibiting bands at 437, 529, and 549 cm^{-1}, respectively. These modes presumably involve deformation of the *tert*-butyl group. The 1103 cm^{-1} band in the unlabeled sample (Figure 5A) shifts significantly to 1084 cm^{-1} in the mixed $^{15}N^tBu$:$^{14}N^tBu$ sample (Figure 5B), and also downshifts slightly (3 cm^{-1}) for the deuterated sample (Figure 5C). Unfortunately, the 1238 cm^{-1} mode in the unlabeled spectrum (Figure 5A) is obscured in the ^{15}N sample. This massive band may be due to partial decomposition of the sample, solvent contamination, or even contaminating $R_3P{=}N^tBu$. The feature at 1238 cm^{-1} in the unlabeled complex (Figure 5A) undergoes a 12 cm^{-1} shift upon deuteration (Figure 5C), consistent with a larger contribution from modes involving deformation of the *tert*-butyl group.

A number of aryl imide complexes supported by the $[PhBP_3]$ ligand are known, and excitation into the low-energy band of $[PhBP_3]Fe{\equiv}NPh$ with 647.1 nm light affords a rich Raman spectrum (Figure 6A). This spectrum has several prominent nonsolvent features at 547, 672, 958, 995, 1163, 1292, 1309, 1339, 1466, and 1573 cm^{-1}. An excitation profile demonstrates that several vibrations are resonance enhanced by excitation into the intense optical transitions associated with the imido moiety (Figure 7). In addition, a number of weakly resonance-enhanced features below 500 cm^{-1} may be metal−ligand deformation modes. The solution spectra show similar features (Figure 8). The band at 1267 cm^{-1} is solvent-derived and appears in the spectrum of the pure solvent. Furthermore, the polarization studies of the lines suggest that the vibrations must have A_1 symmetry. The aryl imides show more complex vibrational spectra than the alkyl imides described above.

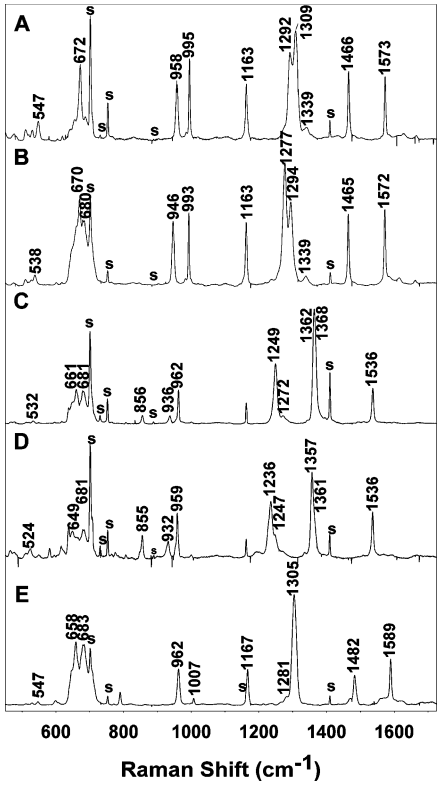

Figure 6. Resonance Raman spectra of (A) $[PhBP_3]Fe{\equiv}NPh$, (B) $[PhBP_3]Fe{\equiv}{}^{15}NPh$, (C) $[PhBP_3]Fe{\equiv}NPh$-d_5, (D) $[PhBP_3]Fe{\equiv}{}^{15}NPh$-$d_5$, and (E) $[PhBP_3]Fe{\equiv}N(p\text{-tolyl})$ in CH_2Cl_2. All spectra were obtained at 77 K using a backscattering geometry (647.1 nm excitation). Peaks due to solvent are marked with an 's'.

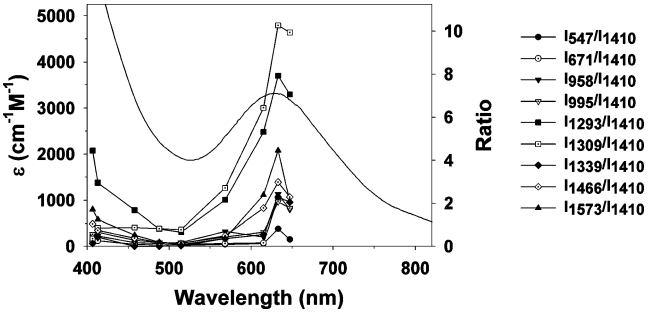

Figure 7. Electronic spectrum of $[PhBP_3]Fe{\equiv}NPh$ in CH_2Cl_2 recorded at room temperature, and resonance Raman excitation profiles for the bands assigned to the compound. The 1410 cm^{-1} dichloromethane vibration was used as the internal standard, and the areas of the peaks were determined by curve fitting.

Isotopic labeling studies were carried out in order to aid in the assignment of the vibrational modes of $[PhBP_3]Fe{\equiv}NPh$ (Figure 6). A number of bands shift in the ^{15}N-labeled sample consistent with significant displacement of the nitrogen atom in those modes (Figure 6B). The only bands which are not affected are the bands at 672, 1163, 1339, 1466, and 1573 cm^{-1}. Deuteration of the phenyl ring significantly alters the spectra with the disappearance of several bands (notably 1163 cm^{-1}) and the appearance of a new band at 856 cm^{-1} (Figure 6C). We have also collected the spectrum of the doubly labeled sample (Figure 6D). The features much more closely resemble those of the deuterated sample. The interpretation of shifts observed for these samples will be discussed below. The spectrum of the

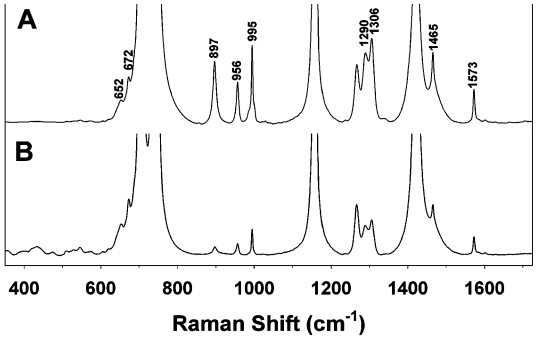

Figure 8. Polarization of (A) [PhBP$_3$]Fe≡NPh in CH_2Cl_2 ($I_{||}$), (B) [PhBP$_3$]Fe≡NPh in CH_2Cl_2($I_\perp$). All spectra were obtained at −55 °C using a spinning cell with a 90° scattering geometry with 647.1 nm excitation.

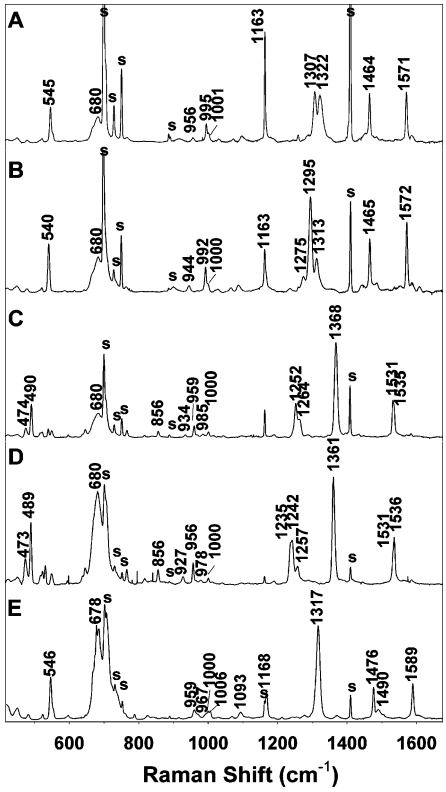

Figure 9. Resonance Raman spectra of (A) [PhBP$_3$]Co≡NPh, (B) [PhBP$_3$]Co≡^{15}NPh, (C) [PhBP$_3$]Co≡NPh-d_5, (D) [PhBP$_3$]Co≡^{15}NPh-d_5, and (E) [PhBP$_3$]Co≡N(*p*-tolyl) in CH_2Cl_2. All spectra were obtained at 77 K using a backscattering geometry (632.8 nm excitation). Peaks due to solvent are marked with an 's'.

analogous [PhBP$_3$]Fe≡N(*p*-tolyl) has also been collected and exhibits modes similar to the phenyl imide (Figure 6E).

Analogous Raman spectra are observed for [PhBP$_3$]Co≡NPh upon excitation with 632.8 nm light (Figure 9). This wavelength was used due to the insensitivity of the complex to excitation wavelength. Several vibrations are observed at 545, 680, 956, 995, 1001, 1163, 1307, 1322, 1464, and 1571 cm^{-1}. A set of isotopically labeled samples (including ^{15}N, Ph-d_5, and the doubly labeled (^{15}N, Ph-d_5)) has been generated and their spectra recorded (Figure 9B−D). Though the cobalt spectra suffer from more noise, the similarity between the features observed in the cobalt and iron complexes is noteworthy. Deuteration of the phenyl ring results in significant changes to the observed spectra which mirror those observed in the iron(III) imides. The shifts of the isotopically labeled samples will be discussed in greater detail below. [PhBP$_3$]Co≡N(*p*-tolyl) exhibits similar resonance Raman spectra (Figure 9E).

Discussion

The optical transitions of early transition metal imides have been extensively studied and typically involve ligand-to-metal charge-transfer transitions.[22,50−52] The trivalent metal imides discussed here also give rise to unique intense optical bands. In both the iron and cobalt complexes, the replacement of the alkyl group with an aryl ring leads to a red-shift in the energies and an increase in the intensity of these transitions (Table 1). This is similar to observations on d^0 imides where higher-energy transitions are observed for alkyl imides than for aryl imides.[50,51] Unlike iron(III) anilides[23,53,54] and iron(III) phenolates,[55−57,58] these pseudo-tetrahedral molecules do not exhibit an appreciable shift upon substitution of the aryl ring. This suggests that the mixing of the arene π system with the M−N π-bonding manifold is not extensive.

The proposed electronic structure of the low-spin trivalent metal imides more closely resembles that of metallocenes. Both spin-allowed d−d transitions and charge-transfer transitions are observed for metallocenes in the visible region.[59,60] Interestingly, the transitions observed in the visible region for the trivalent imides described here have extinction coefficients that would appear to be anomalously high if they correlate with d−d transitions. Circumstantial evidence for assigning the strong band at 640 nm in the iron(III) phenyl imide to a ligand-to-metal charge-transfer transition arises from the sensitivity of Raman features to excitation wavelength (e.g., Fe^{III}NPh, Figure 7). It is interesting to note that the optical spectra of the Fe(III) imides have been recorded in both benzene and methylene chloride and do not appear to show solvatochromism. The spectral features for the cobalt aryl imides and in the metal alkyl imides show less resonance enhancement and are quite different overall from that of the iron arylimide analogue. We are considering the possibility that some of the visible transitions are in fact d−d in character. There is literature precedent to suggest that unusually intense d−d transitions can arise for highly covalent phosphine complexes that have 3-fold symmetry.[61,62]

(50) Heinselman, K. S.; Hopkins, M. D. *J. Am. Chem. Soc.* **1995**, *117*, 12340.
(51) Williams, D. S.; Thompson, D. W.; Korolev, A. V. *J. Am. Chem. Soc.* **1996**, *118*, 6526.
(52) Williams, D. S.; Korolev, A. V. *Inorg. Chem.* **1998**, *37*, 3809.
(53) Jensen, M. P.; Que, L., Jr. Personal communication.
(54) Penkert, F. N.; Weyhermüller, T.; Bill, E.; Hildebrandt, P.; Lecomte, S.; Wieghardt, K. *J. Am. Chem. Soc.* **2000**, *122*, 9663.
(55) Gaber, B. P.; Miskowski, V. M.; Spiro, T. G. *J. Am Chem. Soc.* **1974**, *96*, 6868.
(56) Pyrz, J. W.; Roe, A. L.; Stern, L. J.; Que, L., Jr. *J. Am. Chem. Soc.* **1985**, *107*, 614.
(57) Que, L., Jr. In *Biological Applications of Raman Spectroscopy*; Spiro, T. G., Ed.; John Wiley and Sons: New York, 1988; Vol. 3, p 491.
(58) Jensen, M. P.; Lange, S. J.; Mehn, M. P.; Que, E. L.; Que, L., Jr. *J. Am. Chem. Soc.* **2003**, *125*, 2113.
(59) Sohn, Y. S.; Hendrickson, D. N.; Gray, H. B. *J. Am Chem. Soc.* **1971**, *93*, 3603.
(60) Sohn, Y. S.; Hendrickson, D. N.; Gray, H. B. *J. Am Chem. Soc.* **1970**, *92*, 3233.

Table 3. Summary of Metal Imido Assignments and Comparisons

compound	d_{M-N} (Å)	d_{N-C} (Å)	ν_{M-NR} (cm^{-1})	ν_{MN-R} (cm^{-1})	ref
$[PhBP_3]Fe{\equiv}N^tBu$	1.635(1)	1.442(2)	1104	1233	
$[PhBP_3]Fe{\equiv}N(1\text{-Ad})$	1.641(2)	1.428(3)	1097	1225	37
$[PhBP_3]Co{\equiv}N^tBu$	1.633(2)	1.441(2)	1103	1238	
$[Fe_4(\mu_3\text{-}N^tBu)_4(N^tBu)Cl_3]$	1.635(4)	1.490(6)	1111[a]	1214[a]	49
$Cp^*Ir{\equiv}N^tBu$	1.712(7)	1.45(1)	1033[a]	1258[a]	4
$[PhBP_3]Fe{\equiv}NPh$			958	1292/1309	
$[PhBP_3]Fe{\equiv}N(p\text{-tolyl})$	1.659(2)	1.382(3)	962	1281/1305	27
$[PhBP_3]Co{\equiv}NPh$			956	1307/1332	
$[PhBP_3]Co{\equiv}N(p\text{-tolyl})$	1.658(2)	1.367(2)	959	1317	26
$Cp^*_2V{\equiv}NPh$	1.730(5)	1.345(9)	934	1330	40
$[PhBP^{iPr}_3]Fe{\equiv}N$	1.54	–	1034	–	29,68
$(Mes)_3Ir^V{=}O$	1.725(9)	–	802	–	35
$(TMC)Fe^{IV}{=}O$	1.646(3)	–	834	–	69

[a] New assignment.

An accurate assignment of these transitions is not possible from the data in hand but is now the focus of a separate study.

The resonance Raman spectra of the trivalent iron and cobalt alkyl imido complexes are strikingly similar (Table 2). Both types of imides elicit spectra with bands near 1100 cm^{-1} that downshift ~20 cm^{-1} upon ^{15}N substitution; deuteration of the ^{t}Bu group affects this mode to a lesser extent. We thus assign the 1100 cm^{-1} mode to be primarily composed of a metal−nitrogen stretch, with a smaller contribution from deformations of the *tert*-butyl group. Though it is a gross oversimplification, we will refer to this mode as the metal−nitrogen stretch ($\nu(M{-}N\text{R})$). In addition, both complexes possess a mode near ~1235 cm^{-1} that has less metal−nitrogen stretching character (the iron complex exhibits a downshift of 5 cm^{-1} upon ^{15}N substitution) and is much more responsive to deuteration, giving an ~13 cm^{-1} downshift. We assign this feature to a mode that is mostly comprised of the C−N stretch ($\nu(\text{M}N{-}R)$) of the imido complex. None of the lower-energy features (<600 cm^{-1}) are significantly affected by ^{15}N labeling, though the band at 577 cm^{-1} is affected by deuteration. This mode must involve deformation of the *tert*-butyl group but does not possess a significant metal−nitrogen stretch.

Vibrational features can be identified in the spectra of other metal alkyl imides, which have similarly short metal−nitrogen bond distances and are thought to have multiple-bond character (Tables 2 and 3).[17,19,63] The vibrational features of $Cp^*Ir^{III}{\equiv}N^tBu$ are noteworthy in that three IR bands are reported at 1258, 1071, and 1033 cm^{-1}; iridium−nitrogen multiple bonding was invoked in describing this d^6 complex.[4] Williams and co-workers have commented on the large degree of coupling in $Ta(N^tBu)Cl_3(dme)$ and, though they calculate three features at ~635, 1170, and 1500 cm^{-1}, they were only able to reliably observe features at 1275 and 1586 cm^{-1} using infrared spectroscopy.[21] Isotope-labeling studies have not been carried out for either the tantalum or iridium complexes discussed above. Lee and co-workers observed two weak bands for $[Fe_4(\mu_3\text{-}N^tBu)_4(N^tBu)Cl_3]$ at 955 cm^{-1} and 1262 cm^{-1} that they tentatively assigned as coupled ν(Fe−N) and ν(N−C) modes, but without corroboration by isotope labeling.[49] This cluster formally has a single iron(IV) site and the iron−nitrogen bond lengths for the terminally bound iron imide appear to be comparable to those observed for the mononuclear metal−alkylimido complexes (Table 3). We will return to Lee's original assignment below.

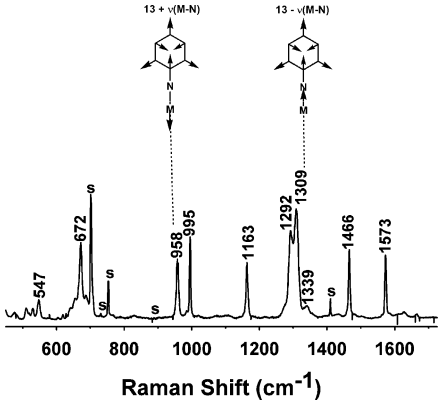

Figure 10. Resonance Raman spectra of $[PhBP_3]Fe{\equiv}NPh$ annotated with hypothetical normal modes for the symmetric and asymmetric combination of iron−nitrogen stretches with the phenyl ring vibrational modes. Peaks due to solvent are marked with an 's.

The resonance Raman spectra of the trivalent metal aryl imides exhibit features from 600 to 1600 cm^{-1}, consistent with a high degree of coupling with the aryl ring vibrational modes (Table 2). For simplicity, we will focus on the iron complexes, though similar trends are observed in the cobalt species. The particular features will be discussed beginning with those with the highest degree of metal−nitrogen stretching character moving to those less affected by ^{15}N substitution. On the basis of literature precedent, we hoped to uncover the symmetric and asymmetric combinations of $\nu(M{-}N\text{R})$ and $\nu(\text{M}N{-}R)$. This is complicated even in the parent aniline species by mixing of the $N{-}C_6H_5$ stretching mode with A_1 modes of the phenyl ring.[64] Two hypothetical vibrational modes are illustrated in Figure 10. These assignments are based upon literature precedent for the vibrational features of metal phenolates,[56,57] metal anilides,[54] and metal alkylidynes.[15,16] The observed spectra are also strikingly similar to those reported for phenolate anion.[65]

(61) Dawson, J. W.; Gray, H. B.; Hix, J. E.; Preer, J. R.; Venanzi, L. M. *J. Am. Chem. Soc.* **1972**, *94*, 2979.
(62) Dyer, G.; Meek, D. W. *Inorg. Chem.* **1967**, *6*, 149.
(63) Rocklage, S. M.; Schrock, R. R. *J. Am Chem. Soc.* **1982**, *104*, 3077.
(64) Varsanyi, G. *Vibrational Spectra of Benzene Derivatives*; Academic Press: New York, 1969.

For $[PhBP_3]Fe{\equiv}NPh$, the largest downshift observed upon ^{15}N substitution arises from the 958 cm^{-1} feature. This 12 cm^{-1} downshift is less than half that predicted for a simple harmonic oscillator (26 cm^{-1}), providing support for strong coupling with the aromatic ring vibrations. Deuteration uncouples the aromatic ring vibration associated with this mode from the metal−nitrogen stretch, resulting in a 4 cm^{-1} upshift to 962 cm^{-1} and the appearance of the phenyl mode at 936 cm^{-1}. Comparison of the doubly labeled complex ($[PhBP_3]Fe{\equiv}^{15}NC_6D_5$, Figure 6D) to the deuterated sample ($[PhBP_3]Fe{\equiv}NC_6D_5$, Figure 6C) shows a modest 3 cm^{-1} downshift; however, it does not approach that observed for the ^{15}N-labeled sample. The 958 cm^{-1} band has the greatest iron−nitrogen stretching character and in this discussion will be denoted as $\nu(Fe{-}N\mathrm{R})$ for simplicity.

The bands near 1300 cm^{-1} also show significant metal−nitrogen stretching character in $[PhBP_3]Fe{\equiv}NPh$. The 1292 and 1309 cm^{-1} features are sensitive to ^{15}N substitution (downshifts of 15 cm^{-1} each) and are also influenced by deuteration (downshifts of 43 and 37 cm^{-1}, respectively). Though these ^{15}N downshifts are larger in magnitude than those described in the preceding paragraph, the percent change is smaller because the shift predicted by a simple harmonic oscillator is larger at higher energy. The doubly labeled sample, $[PhBP_3]Fe{\equiv}^{15}NC_6D_5$, exhibits bands at 1236 and 1247 cm^{-1}. The downshifts observed from the difference spectrum obtained when subtracting Figure 6C from Figure 6D (13 and 25 cm^{-1}, respectively) are similar to the changes observed between the natural-abundance and $[PhBP_3]Fe{\equiv}NC_6D_5$ samples (Figure 6A − Figure 6B). The greater shift for the higher-energy band suggests it has the greater amount of iron−nitrogen stretching character. Given the higher sensitivity to deuteration compared to the lower-energy band discussed above, it seems likely that these bands are coupled to modes of the phenyl ring (possibly ν_{7a} and/or ν_{14}).[65] While the 1309 cm^{-1} band has significant iron−nitrogen stretching character, the higher sensitivity to deuteration argues for its assignment as a mode with predominant $\nu(Fe{N}{-}R)$ character.

Our assignments of these two bands with high Fe−N stretching character (958 and 1309 cm^{-1}) are consistent with the assignments of Osborne and Trogler in their studies of $Cp^*_2V{\equiv}NPh$ ($\nu(V{-}N\mathrm{Ph}) = 934\ cm^{-1}$, $\nu(VN{-}Ph) = 1300\ cm^{-1}$) and support their original proposal that these stretches do not reflect a simple diatomic oscillator.[40,66] Furthermore, the pseudo-tetrahedral low-spin metal−aryl imides examined here show vibrational features similar to those observed for *mer*,*cis*-$M(NAr)X_3L_2$ (M = Ta or Nb).[22] We adopt the proposal of Hopkins and suggest that these modes are a combination of the metal−nitrogen stretching mode and a phenyl ring vibrational mode. Using Varsanyi's benzene notation,[64] Hopkins has suggested the lower-energy band (in our case 958 cm^{-1}) may be assigned to the symmetric combination of the metal−nitrogen stretch and the ν_{13} vibrational mode of the imide phenyl ring. The higher-energy mode (in our case 1309 cm^{-1}) is then the antisymmetric combination ($\nu(\mathrm{M}{-}\mathrm{N})$-$\nu_{13}$). This is also in agreement with the arguments advanced by Dehnicke and Strähle.[39] Griffith and co-workers assigned the lower-frequency band to an asymmetric combination ($\nu(M{-}N\mathrm{R})$-ν_{13}) on the basis of Raman depolarization.[19] As Hopkins has noted,[22] both the symmetric and antisymmetric modes would transform as A_1 and are therefore indistinguishable via depolarization. Our polarization experiments showed (Figure 8) that all of the features we observe are polarized and must transform as A_1, so this holds no further information regarding the assignment of this band. $[PhBP_3]Fe{\equiv}N$(*p*-tolyl) exhibits similar features to those of the phenyl imide, and analogous assignments are made with a slightly higher metal−nitrogen stretch at 962 cm^{-1} and a $\nu(Fe{N}{-}R)$ vibration at lower energy at 1305 cm^{-1} (Figure 6E).

In the Raman spectrum of $[PhBP_3]Fe{\equiv}NPh$, the band at 995 cm^{-1} only shifts by 2 cm^{-1} upon ^{15}N labeling (Figure 6B, Table 2). However, it is very sensitive to deuteration and the band shifts to 856 cm^{-1}. This isotopic sensitivity to deuteration is similar to that observed for the ν_{12} mode of the phenolate anion reported by Spiro and co-workers.[65] We favor this explanation for the appearance of the band at ~856 cm^{-1} in the $-C_6D_5$ samples. Comparison of the deuterated and doubly labeled (^{15}N, ^2H) sample shows almost no ^{15}N sensitivity (Figure 6C and D).

In the Raman spectrum of $[PhBP_3]Fe{\equiv}NPh$, the feature at 1163 cm^{-1} is not affected by nitrogen substitution and is coincident with a CH_2Cl_2 vibration. This band is attenuated upon deuteration (Figure 6C or D). We propose that it is a mode of the phenyl ring which involves only C−H bending or stretching (such as ν_{9a} using the benzene notation[64]). It is interesting to note that the spectrum of $[PhBP_3]Fe{\equiv}N$(*p*-tolyl) exhibits a feature at 1167 cm^{-1} with a shoulder that corresponds to the solvent vibration at 1163 cm^{-1} (Figure 6E).

The two higher-energy bands in the Raman spectrum of $[PhBP_3]Fe{\equiv}NPh$ at 1466 and 1573 cm^{-1} are unaffected by nitrogen substitution but downshift significantly upon deuteration of the phenyl ring (Figure 6C and D), consistent with their assignment as aromatic ring vibrations. Analogous to the vibrations of the isoelectronic phenolate[65] and the spectra of iron(III) phenolate complexes,[56,57] the 1466 cm^{-1} vibration is assigned as $\nu_{19a/b}$, and the 1573 cm^{-1} mode would have the designation $\nu_{8a/b}$.

For $[PhBP_3]Fe{\equiv}NPh$, the 547 cm^{-1} feature downshifts by 9 cm^{-1} upon ^{15}N labeling; however, this vibration must also involve the phenyl ring as the d_5-isotopomer has a feature centered at 532 cm^{-1}. The doubly labeled complex (^{15}N, d_5) corroborates this conclusion: the shift observed between the natural-abundance and the ^{15}N sample (difference of spectra B and A gives a downshift of 9 cm^{-1}) is close to that observed between the deuterated and doubly labeled sample (difference between spectra D and C yields a downshift of 8 cm^{-1}). For $[\{W(NPh)Cl_4\}_2]$, Griffith observed a feature at 683 cm^{-1} that downshifted 5 cm^{-1} upon ^{15}N substitution. We also observe several features centered at 672 cm^{-1} that show a small 2 cm^{-1} downshift upon ^{15}N labeling but change

(65) Mukherjee, A.; McGlashen, M. L.; Spiro, T. G. *J. Phys. Chem.* **1995**, *99*, 4912.
(66) Osborne, J. H.; Rheingold, A. L.; Trogler, W. C. *J. Am. Chem. Soc.* **1985**, *107*, 7945.

drastically upon deuteration. Therefore, we believe these bands also involve phenyl ring modes (perhaps ν_{6a} or ν_1).

The present vibrational study clearly demonstrates that resonance Raman spectroscopy is an effective means to probe the vibrational features of metal imides. While some isotope-labeling experiments have been carried out in the course of previous studies to aid in the assignment of the vibrational features of metal imides, this study represents the most complete set of isotope-labeling studies to date. As one might expect on the basis of the electronic structure models proposed previously,[26,37] the vibrational modes observed for the cobalt and iron imides are surprisingly similar (Figure 9 and Table 2). On the basis of the data given here for mononuclear alkylimido complexes, we can suggest similar assignments for Lee's complex $[Fe_4(\mu_3\text{-}N^tBu)_4(N^tBu)Cl_3]$,[49] though we caution that any such assignments remain to be corroborated by isotopic labeling. Future studies will explore the relationship between changes in oxidation state and the vibrational features (e.g., iron(II) through iron(IV) imides).[37,38]

The observed resonance Raman features are strikingly similar to those observed for metal−alkylidyne complexes (M≡C−R). Prior studies on transition metal−alkylidyne complexes have offered a note of caution for the interpretation of these vibrational features. A thorough investigation of the vibrational spectra of alkyl and aryl alkylidynes (R = Me, Ph) led to the assignment of a high-frequency band (1270−1380 cm^{-1}) as the mode with the greatest metal−carbon stretching character (ν(M≡C)).[14,67] However, this mode is strongly coupled with the symmetric modes of the substituent, and normal coordinate analysis suggests this feature has less than 50% M≡C stretching character.[15,16] Analysis of the parent methylidyne (M≡C−H) revealed a mode at 910 cm^{-1} and led to a much lower force constant, which is a far more accurate measure of the metal−carbon bonding interaction.[15,16] Some care must be exercised in attempting to infer conclusions about bond strength from the vibrational features of the analogous imides, which also give ample evidence of coupling to vibrational features of the ancillary organic group. Attempts are currently underway to obtain parent trivalent imides (M^{III}≡N−H) which, having fewer degrees of freedom and a lower degree of coupling, may simplify the interpretation of the vibrational features.

A priori, one might anticipate a stronger M−N linkage for a nitride than an imide. The higher π-donor capacity of a nitride, as opposed to an imide, has only been demonstrated for complexes of osmium(VIII). For example, OsO_4, OsO_3N^tBu, and $[O_3Os{\equiv}N]^-$ exhibit ν(Os═O) bands at 963 and 956, 925 and 912, and 897 and 871 cm^{-1} respectively.[3] The nitride stretch appears at 1073 cm^{-1}, and $O_3Os{\equiv}N^tBu$ shows a feature at 1184 cm^{-1}, yet the ν(Os═O) vibrational features suggest that the nitride is a better π donor. For comparison, we have recently reported a terminal nitride of iron(IV), with a very short metal−nitrogen bond vector (Table 3) that exhibits an iron−nitrogen stretch at 1034 cm^{-1} in its IR spectrum.[29] Curiously, the stretch observed for $[PhBP^{iPr}_3]Fe^{IV}{\equiv}N$ lies at lower energy than the bands observed for the $[PhBP_3]M{\equiv}NR$ alkyl imides. Despite the observation of vibrations at significantly higher energy for organoimido complexes, the extensive coupling to the A_1 modes of the organic group renders a simple diatomic oscillator description of the $[PhBP_3]M{\equiv}NR$ modes uninstructive in regard to any change in bond strength between a M≡N and a M≡NR species. Therefore, at this stage we cannot quantitatively differentiate the nitride and imide systems without force constants from a complete normal coordinate analysis. Qualitatively, however, we would expect the force constant for the true ν(*Fe*−*N*R) stretch to be shifted to higher energy than the coupled vibration we can experimentally observe. Therefore, we can at least suggest that the ν(*Fe*−*N*R) vibrations of $[BP_3]Fe{\equiv}NR$ systems are higher in energy than the related ν(*Fe*−*N*) vibration of the terminal nitride $[PhBP^{iPr}_3]Fe{\equiv}N$.

To close, the results point to a high degree of multiple-bond character between the metal and the nitrogen nuclei for the trivalent metal imides described here. The degree of coupling to the ancillary organic group appears higher in the aryl imides than in the alkyl imides, but in both cases, we have utilized isotope labeling to arrive at the modes with the greatest degree of metal−nitrogen stretching character. These studies provide a foundation for future work exploring the vibrational features of parent metal imide (M^{III}≡N−H) systems, and studies to probe the degree to which changes in the d-electron count of an imide complex alters the vibrational signatures, at least for pseudo-tetrahedral systems. Finally, as imides of the later first row metals have become attractive synthetic targets in recent years, the data described herein should help in their elucidation by vibrational techniques.

Acknowledgment. This work was supported by the National Institutes of Health at the University of Minnesota (GM-33162 to L.Q. and Predoctoral Traineeship GM-08700 to M.P.M.), and at the California Institute of Technology (GM-070757 to J.C.P. and Postdoctoral Fellowship GM-072291 to M.P.M.). D.M.J. was supported by a National Science Foundation Predoctoral Fellowship. The authors are grateful to Dr. Michael W. Day and Larry M. Henling for technical assistance with the crystallographic portion of this work.

Supporting Information Available: Crystallographic data (pdf and cif). This material is available free of charge via the Internet at http://pubs.acs.org.

IC060670R

(67) Fischer, E. O.; Dao, N. Q.; Wagner, W. R. *Angew. Chem., Int. Ed. Engl.* **1978**, *17*, 50.
(68) Rohde, J.-U.; Betley, T. A.; Peters, J. C.; Que, L. manuscript in preparation.
(69) Rohde, J.-U.; In, J.-H.; Lim, M. H.; Brennessel, W. W.; Bukowski, M. R.; Stubna, A.; Munck, E.; Nam, W.; Que, L., Jr. *Proc. Natl. Acad. Sci. U.S.A.* **2003**, *100*, 3665.